Chapter 2

Multi-IRS-Assisted SISO System Over Rician Fading

In this Chapter, the OP performance of multiple-IRS-assisted SISO wireless system over Rician fading channels, focusing on IRS panel selection is analyzed. Using the CLT and LSE, approximate closed-form expressions for OP are derived. Additionally, a asymptotic OP is derived to determine diversity order and coding gain.

2.1 Introduction

IRS–assisted wireless networks have received substantial attention recently in academic and industry communities for future wireless networks. An IRS panel is made of several reflecting surfaces and each reflecting surface can suitably adjust the phase of the impinging signal. It can also improve the received signal quality and enhances service coverage significantly [56–59]. Thus, the IRS panel uses passive beamforming to retransmit the electromagnetic wave in the desired direction, and as a result, an

IRS-assisted system can mitigate the deep fading scenario by suitably reconfiguring a wireless environment [60–62]. Therefore, the IRS panel enhances the energy efficiency of a wireless system with a higher coverage area and lower latency. Moreover, the hardware/energy cost of an IRS panel is also lower in comparison to traditional active antenna arrays.

In the literature, there are several articles which are studying the performance of IRS-aided wireless communications [26–32, 35, 63–74]. In [26], OP, ASER, and ergodic capacity for a single-IRS system is studied over Rician channels. Samuh et al [27] have also presented the performance of a single IRS system over Nakagami-m fading channels in terms of OP, ASER, and channel capacity. In [28], the ASER expression for several modulation schemes for a single IRS system is obtained over double-Nakagami-m fading channels. The OP, the average received SNR, the ergodic capacity, and the ASER for a single IRS system are also derived over double-Nakagami-m fading channels in [63]. In [29], ASER performance of quadrature amplitude modulation schemes in a single-IRS-aided wireless communication system is studied for Rayleigh fading channels. In [30], a downlink multiple-user scenario with IRS is studied for energy-efficient designs. The ergodic spectral efficiency of an IRS-based wireless communication system is investigated for Rician fading channels in [64]. Authors have investigated achievable multicast rate for an IRS-based multi-antenna multicast system in [65]. In [31], authors have studied the achievable capacity limit of IRS-aided multiple-input-multiple-output communication systems. Basar et al., [32] have presented analytical performance limits of IRS-based communications in Rayleigh fading channels. The coverage probability of an IRS-assisted wireless network is studied using stochastic geometry in [66]. The OP of the IRS-assisted multiple-input-single-output (MISO) system for the Rician fading channel using maximum ratio transmission is derived in [67]. In [68], a downlink system

with IRS is studied where the average rate and ergodic rate are obtained. In [69], the OP, ASER, and achievable capacity rate bounds for the IRS-aided SISO system are presented in Rayleigh fading channels. In [70], the OP and achievable capacity rate for the IRS-aided SISO system is derived for generalized fading channels. In [35], an upper bound of the Shannon capacity, and an approximate expression of the OP are presented for the IRS-aided SISO systems over Rician fading channels. Yildirim et al, [71] have suggested various multiple-IRS-assisted 6G wireless networks to achieve future requirements. The OP and asymptotic sum-rate are studied for multiple-IRS-assisted networks over Rayleigh fading channels in [72]. In [73], a multiple-IRS-assisted system has investigated over Rician fading in terms of the OP which is a function of the phase shifts of all IRSs. Further, recently multiple-IRS-assisted system designs are considered in the literature. However, the aforementioned works do not consider a theoretical analysis of multiple-IRS-assisted SISO wireless systems with an IRS panel selection over independent and non-identically distributed (i.n.i.d.) Rician fading channels. This motivates us to study the OP performance of multiple-IRS-assisted SISO wireless communication systems with an IRS panel selection over i.n.i.d. Rician fading channels.

Contributions: To access the viability of multiple-IRS-assisted wireless communications, we investigate the performance of a multiple-IRS-assisted SISO wireless communication system with an IRS panel selection for i.n.i.d. Rician fading channels. The approximate OP expressions in closed form are derived using both the CLT-based method and the LSE-based method. We also derive a simple asymptotic OP to get diversity order and coding gain. The influence of each system parameter such as the number of reflecting surfaces and IRS panels, the Rician parameter, and the position of the IRS panel on the OP performance are thoroughly investigated.

Moreover, we provide Monte-Carlo simulation results to endorse the presented analytical findings. The derived expressions can be useful guidance for the deployment of multiple-IRS-assisted future wireless networks.

This chapter is structured as follows. The system and channel models are given in Section 2.2. The OP expressions are derived in Section 2.3. Numerically computed OP results are discussed in Section 2.4. Section 2.5 concludes the summary of the proposed work. An appendix is given in Section A.

2.2 System and Channel Models

We have considered a SISO communication system that is made of a single-antenna transmitting (Tx) node, and a single-antenna receiving (Rx) node as depicted in Figure 2.1. Assuming that the received signal is coming from different uncorrelated

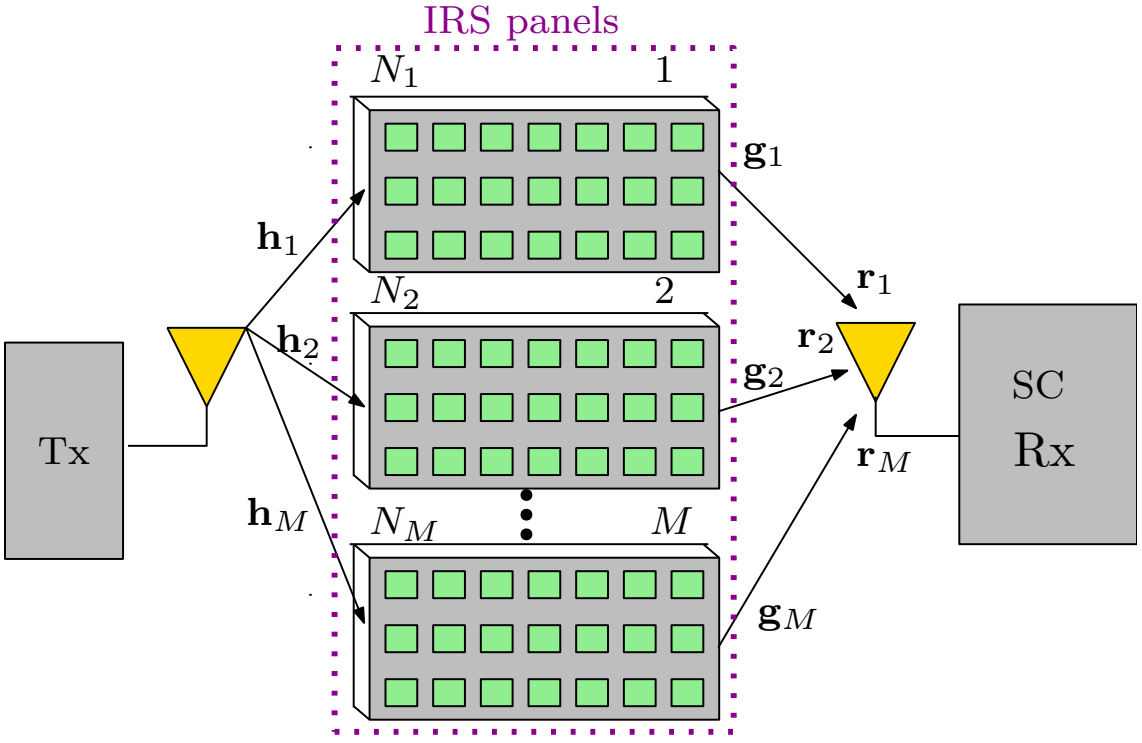

FIGURE 2.1: Multiple-IRS-aided SISO communication system with SC receiver.

paths is having different delays. Further, we also assume that M IRS panels with their controller unit are used to assist the end-to-end communication and each panel has N_m reflecting elements, where $1 \leq m \leq M$. It is considered that the full knowledge of channel state information (CSI) is available at the transceiver. Thus, we can do passive beamforming design by adjusting the phase shift of each element in each IRS panel. However, it is also assumed that the direct link between the Tx node and the Rx node is subjected to deep fading, hence it has been neglected in this work. Thus, the single receiving antenna at the Rx node receives only a signal from each IRS panel. This wireless communication scenario model is a typical application of the uplink scenarios for future cellular wireless systems. The m^{th} received signal r_m at the receiving antenna is given as [32]

$$r_m = \sqrt{P}\left(\mathbf{g_m}^T \mathbf{\Theta_m} \mathbf{h_m}\right) x_t + n_m, \quad 1 \leq m \leq M \tag{2.1}$$

where x_t is the transmitted message with unit energy, P is the transmit power of message x_t, $\mathbf{h_m} = [\mathrm{h}_{m1}, \mathrm{h}_{m2}, \ldots \mathrm{h}_{mN_m}]^T$ and $\mathbf{g_m} = \left[\mathrm{g}_{m1}, \mathrm{g}_{m2}, \ldots \mathrm{g}_{mN_m}\right]^T$ are the vectors of channel coefficients between the Tx node to the m^{th} IRS panel and the m^{th} IRS panel to the receiving antenna of Rx node, respectively, the phase shifts introduced by the reflecting elements of the m^{th} IRS panels are given as a diagonal matrix $\mathbf{\Theta_m} = \mathrm{diag}\{[e^{j\theta_{m1}}, e^{j\theta_{m2}}, \ldots\ldots\ldots, e^{j\theta_{mN_m}}]\}$, and n_m is a zero mean additive white Gaussian noise with variance N_0 at the receiving antenna. Since the IRS panels are located at the LoS to both the Tx node and Rx node; thus, $h_{mi}, 1 \leq i \leq N_m$ are modeled by Rician distribution with Rician parameters K_{h_m} for the m^{th} IRS panel. Therefore, the channel coefficients between the Tx node and the m^{th} IRS panel can

be written as [35]

$$h_{mi} = \frac{1}{\sqrt{d_{h_m}^{\alpha_{h_m}}}} \left(\sqrt{\frac{K_{h_m}}{K_{h_m}+1}} \tilde{h}_{mi} + \sqrt{\frac{1}{K_{h_m}+1}} \hat{h}_{mi} \right), \quad 1 \leq m \leq M \text{ and } 1 \leq i \leq N_m \tag{2.2}$$

where d_{h_m} and α_{h_m} denote the distance and path loss exponent (PLE) for the ith channel between the Tx node and the corresponding m^{th} IRS, respectively. Also, $\tilde{h}_{mi}$ and $\hat{h}_{mi}$ are the normalized LoS and NLoS components for the ith channel between the Tx node and the corresponding m^{th} IRS, respectively. Similarly, $\mathrm{g}_{mi}, 1 \leq i \leq N_m$ are modeled by Rician distribution with Rician parameter K_{g_m} for the m^{th} IRS panel, the channel coefficients between the m^{th} IRS panel and the receiving antenna can be written as [35]

$$\mathrm{g}_{mi} = \frac{1}{\sqrt{d_{\mathrm{g}_m}^{\alpha_{\mathrm{g}_m}}}} \left(\sqrt{\frac{K_{\mathrm{g}_m}}{K_{\mathrm{g}_m}+1}} \tilde{\mathrm{g}}_{mi} + \sqrt{\frac{1}{K_{\mathrm{g}_m}+1}} \hat{\mathrm{g}}_{mi} \right), \quad 1 \leq m \leq M \text{ and } 1 \leq i \leq N_m \tag{2.3}$$

where d_{g_m} and α_{g_m} denote the distance and PLE for the ith channel between the m^{th} IRS and the receiving antenna, respectively. Also, $\tilde{\mathrm{g}}_{mi}$ and $\hat{\mathrm{g}}_{mi}$ are the normalized LoS and NLoS components for the ith channel between the m^{th} IRS and the receiving antenna, respectively.

Assuming that the channel phases are available to each IRS panel controller, applying the optimal co-phasing matrix $\mathbf{\Theta_m}$, the instantaneous optimal SNR γ_m of m^{th} received signal is given by [32]

$$\gamma_m = \gamma_0 \left(\sum_{i=1}^{N_m} |h_{mi}| \, |\mathrm{g}_{mi}| \right)^2, \tag{2.4}$$

where $\gamma_0 = \frac{P}{N_0}$ represents the transmit SNR. Note that it has been considered that the IRS panel which provides the highest instantaneous end-to-end SNR is selected to assist the communication between the Tx node and the Rx node. Thus, the output SNR γ_{sc} at the Rx node can be given as [72]

$$\gamma_{sc} = \max_{1 \leq m \leq M} \{\gamma_m\}. \tag{2.5}$$

2.3 Outage Probability Analysis

In this section, we have derived the approximate OP, the asymptotic OP, the diversity order, and the coding gain of the considered SISO system over i.n.i.d. Rician channels.

The OP of the considered SISO communication system with the best IRS panel selection is given as [8]

$$\begin{aligned} P_{\text{out}} &= \Pr\left(\gamma_{sc} \leq \gamma_{th}\right) \\ &= \Pr\left(\max_{1 \leq m \leq M} \{\gamma_m\} \leq \gamma_{th}\right) \\ &= \prod_{m=1}^{M} F_{\gamma_m}\left(\gamma_{th}\right), \end{aligned} \tag{2.6}$$

where $\Pr(\cdot)$ is a probability operator, $F_{\gamma_m}(\cdot)$ denotes the CDF of instantaneous SNR γ_m and γ_{th} is a predefined threshold SNR. Thus, one needs to derive an expression of $F_{\gamma_m}(\cdot)$ to obtain the OP expression.

2.3.1 Approximate OP Expression

The instantaneous SNR of the m^{th} received signal which is given in (2.4) can be re-expressed as

$$\gamma_m = \mathcal{A}_m^2 \gamma_0, \tag{2.7}$$

where $\mathcal{A}_m = \sum_{i=1}^{N_m} z_{mi}$ and $z_{mi} = |h_{mi}|\,|\mathrm{g}_{mi}|$. We assume that the random variables (RVs) z_{mi} are independent and identically distributed (i.i.d.) RVs which is related to the m^{th} IRS panel. As we know that $|h_{mi}|$ and $|\mathrm{g}_{mi}|$ are i.n.i.d. Rician distributed RVs. To the best of the authors' knowledge, it is not possible to derive an exact tractable closed-form expression for $F_{\gamma_m}(\cdot)$. However, one can approximate $F_{\gamma_m}(\cdot)$ using either the CLT-based method or the LSE-based method.

2.3.1.1 CLT-Based Method

For a large value of N_m, i.e., $N_m >> 1$, with the aid of the CLT method, the RV $\mathcal{A}_m$ can be modeled as a normal distributed RV with the following mean μ_m and standard deviation σ_m [35]:

$$\mu_m = \mathbf{E}[\mathcal{A}_m] = \frac{N_m \pi L_{0.5}(-K_{h_m}) L_{0.5}\left(-K_{\mathrm{g}_m}\right)}{4\sqrt{d_{h_m}^{\alpha_{h_m}} d_{\mathrm{g}_m}^{\alpha_{\mathrm{g}_m}} (K_{h_m}+1)\left(K_{\mathrm{g}_m}+1\right)}}, \tag{2.8}$$

$$\sigma_m^2 = \mathbf{Var}(\mathcal{A}_m) = \frac{N_m}{d_{h_m}^{\alpha_{h_m}} d_{\mathrm{g}_m}^{\alpha_{\mathrm{g}_m}}}\left[1 - \frac{\pi^2 L_{0.5}^2(-K_{h_m}) L_{0.5}^2\left(-K_{\mathrm{g}_m}\right)}{16(K_{h_m}+1)\left(K_{\mathrm{g}_m}+1\right)}\right], \tag{2.9}$$

where $\mathbb{E}[\cdot]$ is the statistical averaging operator, $\mathbf{Var}(\cdot)$ is the statistical variance operator, and $L_m(\cdot)$ denotes the Laguerre polynomial of degree m [75]. Hence, the

CDF of $\mathcal{A}_m$ can be given as [9]

$$F_{\mathcal{A}_m}(x) = 1 - \Theta_m Q\left(\frac{x - \mu_m}{\sigma_m}\right), \tag{2.10}$$

where $\Theta_m = \left(0.5 + 0.5\text{erf}\left(\sqrt{\frac{\mu_m}{2\sigma_m^2}}\right)\right)^{-1}$, $\text{erf}(\cdot)$ is the error function and the Gaussian Q-function is denoted as $Q(\cdot)$ [9]. Now, one can get the CDF of γ_m as the following

$$F_{\gamma_m}(x) = \Pr(\gamma_m \leq x) = \Pr\left(\mathcal{A}_m^2 \gamma_0 \leq x\right) = 1 - \Theta_m Q\left(\frac{\sqrt{\frac{x}{\gamma_0}} - \mu_m}{\sigma_m}\right) \tag{2.11}$$

2.3.1.2 LSE-Based Method

The first-term expansion of $\mathcal{A}_m$ in the LSE method provides a close approximation of its PDF as [26, 76]

$$f_{\mathcal{A}_m}(x) = \frac{x^{\theta_1} \exp\left(-\frac{x}{\theta_2}\right)}{\theta_2^{\theta_1+1}\Gamma(\theta_1+1)}; \tag{2.12}$$

where $\theta_1 = \frac{\mu_m^2}{\sigma_m^2} - 1$ and $\theta_2 = \frac{\sigma_m^2}{\mu_m}$. The CDF expression of $\mathcal{A}_m$ can be written as

$$F_{\mathcal{A}_m}(x) = \int_0^x f_{\mathcal{A}_m}(t)dt = \frac{\gamma\left(\theta_1 + 1, \frac{x}{\theta_2}\right)}{\Gamma(\theta_1 + 1)}, \tag{2.13}$$

where $\gamma(\cdot,\cdot)$ denotes the lower incomplete gamma function [77, (8.350.1)]. Now, one can get the CDF of γ_m as the following

$$F_{\gamma_m}(x) = \Pr(\gamma_m \leq x) = \Pr\left(\mathcal{A}_m^2 \gamma_0 \leq x\right) = \frac{\gamma\left(\theta_1 + 1, \frac{\sqrt{\frac{x}{\gamma_0}}}{\theta_2}\right)}{\Gamma(\theta_1 + 1)} \tag{2.14}$$

Using either (2.11) or (2.14) into (2.6), the approximate OP of the considered SISO wireless system can be obtained as

$$P_{\text{out}} \simeq \prod_{m=1}^{M} F_{\gamma_m}(\gamma_{th}) = \begin{cases} \prod_{m=1}^{M} \left(1 - \Theta_m Q\left(\frac{\sqrt{\frac{\gamma_{th}}{\gamma_0}} - \mu_m}{\sigma_m}\right)\right), & \text{CLT-Based Method} \\ \prod_{m=1}^{M} \frac{\gamma\left(\theta_1+1, \frac{\sqrt{\frac{\gamma_{th}}{\gamma_0}}}{\theta_2}\right)}{\Gamma(\theta_1+1)}, & \text{LSE-Based Method} \end{cases} \tag{2.15}$$

2.3.2 Asymptotic OP Expression

To obtain the asymptotic OP expression, assuming each link is subjected to high SNR $\bar{\gamma}_m = \mathbb{E}[\gamma_m] \to \infty$, where $\mathbb{E}[\cdot]$ is a statistical averaging operator. Using [78, (22)], an approximate asymptotic PDF expression of RV $z_{mi} = |h_{mi}||\mathrm{g}_{mi}|$ can be obtained as

$$f_{z_{mi}}^{\infty}(x) \approx 4\Delta\, d_{h_m}^{\alpha_{h_m}} d_{\mathrm{g}_m}^{\alpha_{\mathrm{g}_m}} \left(1 + K_{h_m}\right)\left(1 + K_{\mathrm{g}_m}\right) x \exp\left(-\left(K_{h_m} + K_{\mathrm{g}_m}\right)\right). \tag{2.16}$$

Note that the details of derivation are given as an appendix in Section A. Further, the corresponding asymptotic moment generating function (MGF) of RV z_{mi} can be given by

$$\begin{aligned} \mathcal{M}_{z_{mi}}^{\infty}(s) &= \int_0^{\infty} \exp(-s\,x)\, f_{z_{mi}}^{\infty}(x)\, dx \\ &= 4\Delta\, d_{h_m}^{\alpha_{h_m}} d_{\mathrm{g}_m}^{\alpha_{\mathrm{g}_m}} \left(1 + K_{h_m}\right)\left(1 + K_{\mathrm{g}_m}\right) \exp\left(-\left(K_{h_m} + K_{\mathrm{g}_m}\right)\right) s^{-2}. \end{aligned} \tag{2.17}$$

Without a loss of generality, we assume that the RVs z_{mi} are i.i.d. RVs which are related to the m^{th} IRS panel. Hence, the MGF expression of $\mathcal{A}_m = \sum_{i=1}^{N_m} z_{mi}$ can be

written as

$$\mathcal{M}_{\mathcal{A}_m}^{\infty}(s) = \prod_{i=1}^{N_m} \mathcal{M}_{z_{mi}}^{\infty}(s) = \left(\mathcal{M}_{z_{mi}}^{\infty}(s)\right)^{N_m} = \lambda_m s^{-2N_m}, \tag{2.18}$$

where $\lambda_m = \left(4\Delta\, d_{h_m}^{\alpha_{h_m}} d_{\mathrm{g}_m}^{\alpha_{\mathrm{g}_m}} \left(1+K_{h_m}\right)\left(1+K_{\mathrm{g}_m}\right)\right)^{N_m} \exp\left(-N_m\left(K_{h_m}+K_{\mathrm{g}_m}\right)\right)$. Taking the inverse Laplace transform of $s^{-1}\mathcal{M}_{\mathcal{A}_m}^{\infty}(s)$, one can obtain the CDF expression of $\mathcal{A}_m$ as

$$F_{\mathcal{A}_m}^{\infty}(x) = \frac{\lambda_m x^{2N_m}}{\Gamma(2N_m+1)}, \tag{2.19}$$

where $\Gamma(\cdot)$ denotes the Gamma function. Hence, one can get the CDF of γ_m as

$$\begin{aligned} F_{\gamma_m}^{\infty}(x) &= \Pr\left(\gamma_m \le x\right) = \Pr\left(\mathcal{A}_m^2\gamma_0 \le x\right) \\ &= \frac{\lambda_m x^{N_m}}{\Gamma(2N_m+1)\gamma_0^{N_m}}. \end{aligned} \tag{2.20}$$

Putting (2.20), into (2.6) the OP of the considered SISO wireless system can be given by

$$P_{\mathrm{out}}^{\infty} = \frac{\gamma_{th}^{\sum_{m=1}^{M} N_m}}{\gamma_0^{\sum_{m=1}^{M} N_m}} \prod_{m=1}^{M} \left(\frac{\lambda_m}{\Gamma(2N_m+1)}\right). \tag{2.21}$$

2.3.3 Diversity Order and Coding Gain

The asymptotic OP can be re-written as [13]

$$P_{\mathrm{out}}^{\infty} = \left(\mathcal{G}_c\gamma_0\right)^{-\mathcal{G}_d}. \tag{2.22}$$

In (2.22), the diversity order is denoted as $\mathcal{G}_d$ and the coding gain is denoted as $\mathcal{G}_c$. From (2.21), we get the following

$$\mathcal{G}_d = \sum_{m=1}^{M} N_m \tag{2.23}$$

and

$$\mathcal{G}_c = \gamma_{th}^{-1} \left(\prod_{m=1}^{M} \left(\frac{\lambda_m x^{N_m}}{\Gamma(2N_m+1)\gamma_0^{N_m}} \right) \right)^{-\frac{1}{\sum_{m=1}^{M} N_m}}. \tag{2.24}$$

2.4 Numerical and Simulation Results

In this section, the considered communication system is analyzed with the help of our derived OP expressions. The Monte-Carlo simulations are also presented to validate our derived OP expressions. For convenient presentation, we assume the following assumption for parameters: $K_{h_m} = K_1, K_{g_m} = K_2, d_{h_m} = d_1, d_{g_m} = d_2, \alpha_{h_m} = \alpha_1, \alpha_{g_m} = \alpha_2, \forall m$. We choose a sub-6G scenario, where the bandwidth of system is 180 KHz, the power spectral density of noise is -173 dBm/Hz, the distances (in meters) are taken to be $d_1 = d_2 = 150$ m, the PLEs are $\alpha_1 = \alpha_2 = 2$, the fading parameters are set to be $K_1 = K_2 = K = 1$, the reference path loss at the reference distance $d_0 = 1$ m is taken to be -30 dB, and the threshold SNR is taken to be $\gamma_{th} = 10$ dB. In each figure, the OP performance is plotted against transmitted power P (dBm). The above set of parameters is also taken for the numerical and the simulation results unless it is stated exclusively.

Figure 2.2 and Figure 2.3 depict the OP performance as a function of P, M, and N_m. Both methods' accuracy (CLT and LSE) is illustrated by utilizing these two figures. Figure 2.2 demonstrates that for small N, the CLT-based approximation

method is not a more accurate approximation. However, for large N, the CLT-based approximation method is closely matched with simulation, like the LSE-based approximation method, as observed in Figure 2.3. The simulation results are matching closely with the analytical results. As expected, the OP decreases when either P or M or N_m is increasing. One can notice that the OP performance improves sharply when either P or M or N_m increases sharply. The multiple-IRS-assisted SISO system outperforms the single IRS-assisted SISO system model, as expected. For example, consider Figure 2.3, at a fixed $P\text{out} = 10^{-3}$, 2 dB of the transmit power gain is observed by varying M from 1 to 2 for a fixed $N = 32$, however, 6.8 dB of the transmit power gain is observed by varying N_m from 32 to 64 for a fixed $M = 2$.

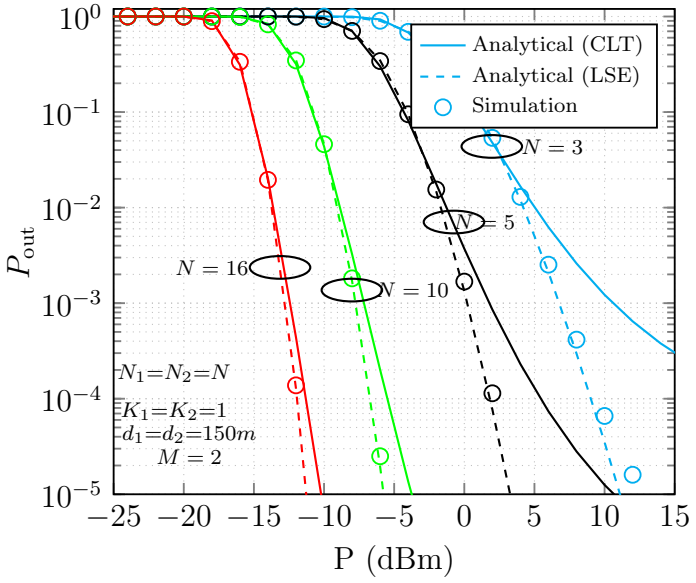

FIGURE 2.2: OP performance with varying N for $M = 2$. The marker, solid and dashed lines denote the simulation, analytical (CLT), and analytical (LSE) results, respectively.

Figures 2.4 and 2.5 are presented to confirm the accuracy of asymptotic OP expression at the high SNR region. It can be observed that the asymptotic OP is approaching the exact OP. Thus, it validates the accuracy of P_{out}^{∞} expression. Moreover, it can also get the diversity order from the slope of the asymptotic OP curves, which

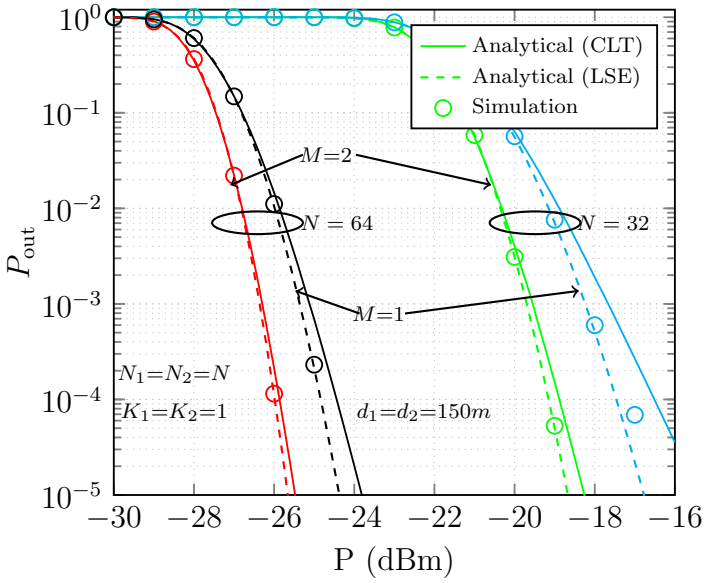

FIGURE 2.3: OP performance with varying both M and N_m. The marker, solid, and dashed lines denote the simulation, analytical (CLT), and analytical (LSE) results, respectively.

is $\sum_{m=1}^{M} N_m$. Moreover, the asymptotic OP for different values of $N = 3, 5, 10, 16$ is matched to the analytical (LSE) results at high SNR, as shown in Figure 2.5.

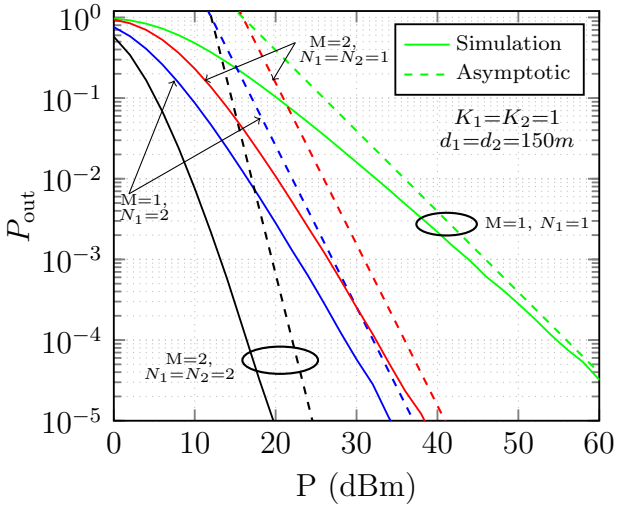

FIGURE 2.4: Asymptotic OP performance with varying both N_m and M. The solid lines and dashed lines denote the simulation and analytical results, respectively.

Figure 2.6 shows the OP performance as a function of the Rician factor $K_{h_m} = K_{g_m} = K$ and P. The OP performance improves with an increase in K because the

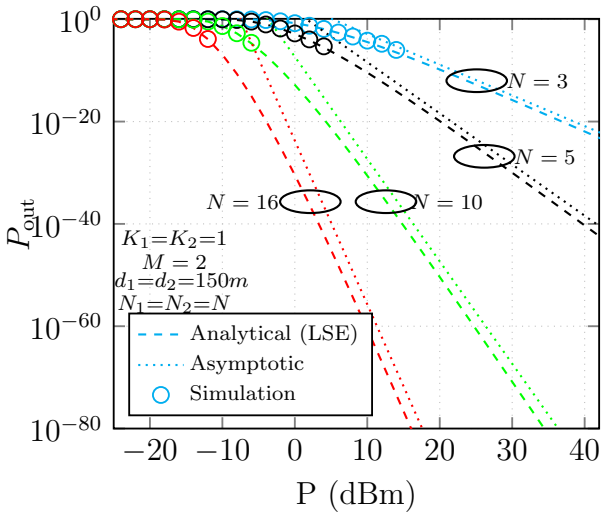

FIGURE 2.5: OP performance with varying N for $M = 2$. The dashed and dotted lines denote the analytical (LSE) and asymptotic results, respectively.

fading severity decrease with an increase in K. For example, at fixed $P\text{out} = 10^{-2}$, a 2.5 dB of the transmit power gain is obtained when K increases from 0 to 5.

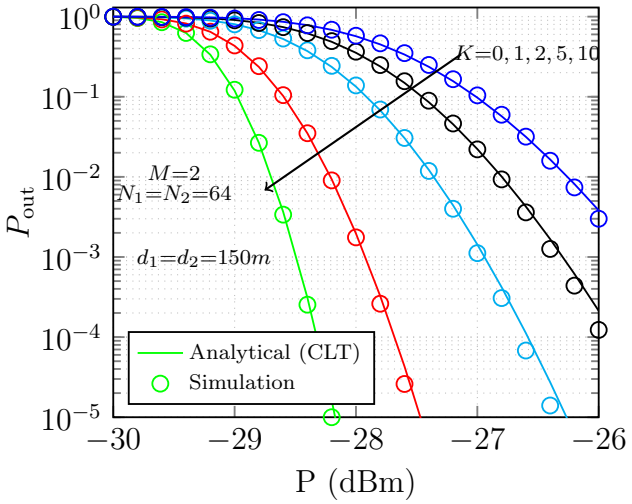

FIGURE 2.6: OP performance with varying K. The solid lines and marker denote the analytical and simulation results, respectively.

Figure 2.7 is presented to study the influence of M on the OP performance. We observe from this figure that as M is increased, the OP performance improves because

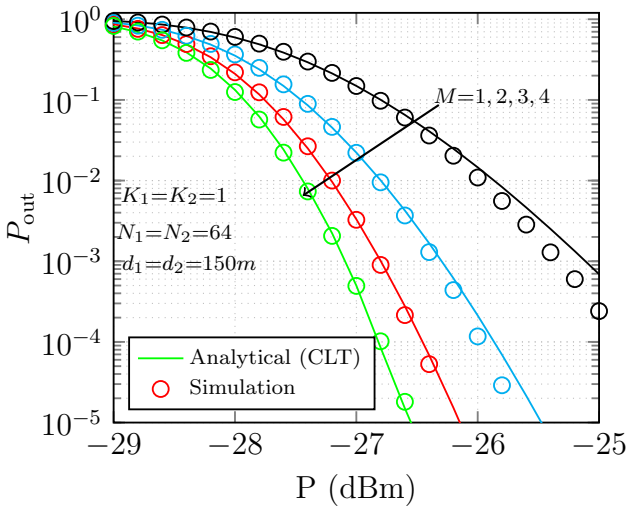

FIGURE 2.7: OP performance with varying M. The solid lines and marker denote the analytical and simulation results, respectively.

of the higher diversity order. For example, at $P_{\text{out}} = 10^{-3}$ as we increase $M = 1$ to $M = 4$ we can observe the performance enhancement of around 2 dB in terms of P.

Next, Figure 2.8 illustrates the influence of the placement of IRS panels between the Tx and Rx on the OP performance with a fixed total distance of 300m ($d_1 + d_2 =$ 300m). We have plotted the OP performance w.r.t the distance d_1 for different values of P. As P increases, the OP performance improves, as shown in Figure 2.8. It can also be noted that the OP decreases when IRS panels are placed closer to either the TX node or Rx node. The reason is that the IRS panels placed closer to either the TX node or Rx node has small path loss. The OP performance is symmetric about the equidistant position ($d_1 = 150$). Further, OP performance is worst at the equidistant position as compared to any other positions, as shown in Figure 2.8.

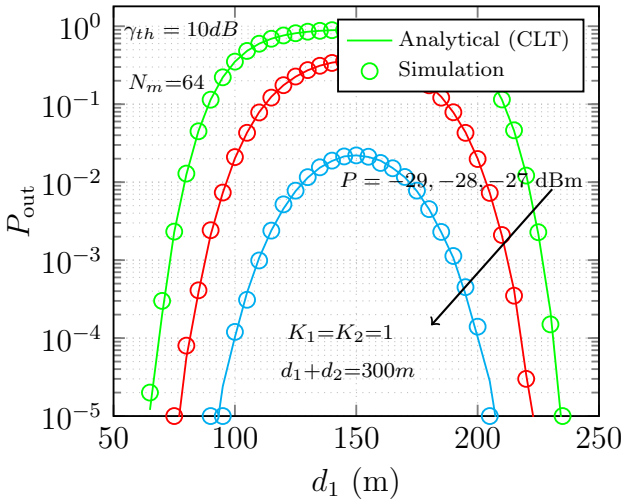

FIGURE 2.8: OP performance w.r.t d_1 for $M = 2$ and fixed $N_m = 64$. The solid lines and marker denote the analytical and simulation results, respectively.

2.5 Summary

In this chapter, the OP performance of multiple-IRS-assisted SISO communication system with the best IRS panel selection has been comprehensively studied for i.n.i.d. Rician fading channels. The approximate OP expressions have been presented in closed form with the aid of both the CLT-based method and the LSE-based method. In addition, the asymptotic OP expression has been also obtained which gives the diversity gain and the coding gain expressions. All analytical expressions have been evaluated to demonstrate the system's performance. Observations indicate that the LSE-based approximation is precise for low values of IRS elements. Additionally, for high values of IRS elements, the LSE-based approximation exhibits a close match with the CLT-based approximation. The influence of the number of IRS elements, the number of IRS panels, the location of the IRS panel, and the fading parameter have been studied. The Monte-Carlo simulation results have been also given to endorse the presented theoretical analysis. The presented results show that the multiple-IRS enhances system performance significantly as compared to a single IRS-assisted system.